Characterization of local gut microbiome and intestinal transcriptome responses to rosiglitazone treatment in diabetic *db/db* mice

Mette Simone Aae Madsen [a,b,*], Rikke Veggerby Grønlund [a], John Eid [c], Mikkel Christensen-Dalsgaard [a], Morten Sommer [b], Kristoffer Rigbolt [a], Martin Rønn Madsen [a], Jacob Jelsing [a], Niels Vrang [a], Henrik H. Hansen [a], Martin Mikkelsen [a]

[a] *Gubra, Hørsholm, Denmark*
[b] *Novo Nordisk Foundation Center for Biosustainability, Technical University of Denmark, Kgs. Lyngby, Denmark* [c] *Pendulum, San Francisco, CA, USA*

ARTICLEINFO

Keywords:
Peroxisome proliferator-activated receptor-γ
Diabetes
Mouse model
Gut microbiome
Gut transcriptome
Gut segment

ABSTRACT

The gut microbiota has been implicated in the therapeutic effects of antidiabetics. It is unclear if antidiabetics directly influences gut microbiome-host interaction. Oral peroxisome proliferator-activated receptor-γ (PPAR-γ) agonists, such as rosiglitazone, are potent insulin sensitizers used in the treatment of type 2 diabetes (T2D). PPAR-γ is abundantly expressed in the intestine, making it possible that PPAR-γ agonists directly influences gut microbiome-host homeostasis. The presented study therefore aimed to characterize local gut microbiome and intestinal transcriptome responses in diabetic *db/db* mice following rosiglitazone treatment. Diabetic B6.BKS(D)- Lepr^{db}/J (*db/db*) mice (8 weeks of age) received oral dosing once daily with vehicle (n = 12) or rosiglitazone (3 mg/kg, n = 12) for 8 weeks. Gut segments (duodenum, jejunum, ileum, caecum, and colon) were sampled for paired analysis of gut microbiota and host transcriptome signatures using full-length bacterial 16S rRNA sequencing and RNA sequencing (n = 5–6 per group). Treatment with rosiglitazone improved glucose homeostasis without influencing local gut microbiome composition in *db/db* mice. In contrast, rosiglitazone promoted marked changes in ileal and colonic gene expression signatures associated with peroxisomal and mitochondrial lipid metabolism, carbohydrate utilization and immune regulation. In conclusion, rosiglitazone treatment markedly affected transcriptional markers of intestinal lipid metabolism and immune regulation but had no effect on the gut microbiome in diabetic *db/db* mice.

1. Introduction

There is an increasing focus on the potential contributory mechanistic role of the gut microbiota in the metabolic effects of glucoregulatory and weight loss promoting drugs [1–4]. Pharmacological treatment of T2D focus on re-establishing glycaemic control using glucose-lowering and insulin sensitizing drugs such as metformin, DPP-4 inhibitors, GLP-1 receptor agonists and selective peroxisome proliferator-activated receptor-gamma (PPAR)-γ agonists, also termed thiazolidinediones (TZDs) [5,6].

PPAR-γ is a ligand-activated transcription factor belonging to a family of nuclear hormone receptors for which lipids and their metabolic products are endogenous ligands [7–10]. By forming a heterodimer with retinoid X receptors (RXR), nuclear PPAR-γ regulates the expression of a large variety of genes involved in lipid and carbohydrate metabolism [9, 11]. Notably, PPAR-γ activation upregulates genes that stimulate insulin signaling as well as transport and disposal of fatty acids [8]. In addition to prominent effects of PPAR-γ on glucose and lipid metabolism in adipose, hepatic and muscle tissue [8,9], the intestine express PPAR-γ and gut microbiota-host interaction through PPAR-γ signalling has been proposed to play a role in gut metabolism and homeostasis [12–14]. For example, fermentation end products of dietary fibers by the intestinal microbiota can activate PPAR-γ signaling in intestinal endothelial cells, which links gut microbiota-host crosstalk to intestinal PPAR-γ signaling [12,15–18]. In addition to a prominent role in nutrient metabolism, PPAR-γ influences intestinal immune responses by regulating the recruitment and activity of various immune cell populations of the innate and adaptive immune system [19]. These effects are considered to limit intestinal pro-inflammatory responses which may contribute to maintain intestinal barrier integrity by sustaining tolerance to commensals [18,20,21]. Accordingly, PPAR-γ agonists reduce the release of pro-inflammatory cytokines and suppress NF-κB signalling pathways in gut epithelial cells [22–25]. Also, anti-inflammatory effects of PPAR-γ agonists have been demonstrated in animal models of gut inflammatory diseases [26,27].

There is an increasing appreciation that obesity and T2D is associated with altered composition and

Abbreviations: DEG, differentially expressed gene; HbA1c, hemoglobin A1c; OGTT, oral glucose tolerance test; PCA, principal component analysis; PCoA, principal coordinate analysis; PPAR-γ, peroxisome proliferator-activated receptor-γ; rRNA, ribosomal RNA; TZD, thiazolidinedione; T2D, type 2 diabetes.

* Corresponding author at: Gubra, Hørsholm Kongevej 11B, DK-2970, Hørsholm, Denmark. *E-mail address:* msm@gubra.dk (M.S.A. Madsen).

https://doi.org/10.1016/j.biopha.2020.110966
Received 12 August 2020; Received in revised form 21 October 2020; Accepted 1 November 2020
Available online 7 November 2020
0753-3322/© 2020 The Author(s). Published by Elsevier Masson SAS. This is an open access article under the CC BY-NC-ND license (http://creativecommons.org/licenses/by-nc-nd/4.0/).

activity of gut bacteria involved in nutrient metabolism, dietary energy harvest and host immune responses [19,21,28,29]. PPAR-γ is abundantly expressed in the intestine, making it possible that oral TZDs modulate gut microbiome-host dynamics which may potentially contribute to the therapeutic effects of this drug class. To investigate a potential gut effect of TZDs in the context of diabetes, we therefore characterized local gut microbiome gene and host transcriptome responses to long-term treatment with rosiglitazone, a standard TZD [5,6], in diabetic *db/db* mice.

2. Materials and methods

2.1. Animals

Eight weeks-old male B6.BKS(D)-Lepr^{db}/J (*db/db*) mice (Janvier Labs, Saint Berthevin, Cedex, France) were housed in a controlled environment (12 h light/dark cycle, lights on/off at 3AM/3 P M; 22 ± 1 °C; 50 ± 10 % relative humidity). All animals were pair-housed, each identified by an implantable microchip (PetID Microchip, E-vet, Haderslev, Denmark). Mice were fed chow (Purina 5008, 3.31 kcal/g, LabDiet, St. Louis, MO) and received domestic quality tap water *ad libitum*. All animal experiments were approved by the Danish Committee for Animal Research using internationally accepted principles for the use of laboratory animals (license no. 2013-15-2934− 00784).

2.2. Drug treatment

Rosiglitazone was acquired from Sigma-Aldrich (St. Louis, MO). Vehicle was phosphate-buffered saline with 0.1 % Tween-80 (pH 7.4). Animals were randomized to treatment (n = 12 per group) according to body weight, 4 h fasted blood glucose and HbA1c levels. Animals were perorally administered vehicle (5 mL/kg) or rosiglitazone (3.0 mg/kg) once daily for a total of 55 days. Body weight and food intake were measured daily during the treatment period.

2.3. Oral glucose tolerance test

Oral glucose tolerance tests (OGTT) were performed on treatment days 28 and 49. Animals were fasted for 4 h prior to the OGTT. Vehicle and rosiglitazone were administered after the OGTT. At time t = 0, a bolus of glucose (2 g/kg, 10 mL/kg, Fresenius Kabi, Uppsala, Sweden) was administered by oral gavage. Tail vein blood samples were collected in 10 μl heparinized capillary tubes at t = − 60, 0, 15, 30, 60, 120 and 180 min, and immediately suspended in glucose/lactate solution buffer (0.5 mL, EKF-diagnostics, Cardiff, UK). Blood glucose concentrations were measured using a BIOSEN C-Line glucose meter (EKF-diagnostics, Barleben, Germany) according to the manufacturer's instructions.

2.4. Plasma biochemistry

Blood glucose levels were measured once weekly in tail blood samples from 4 h fasted mice. Animals were terminated by cardiac puncture under isoflurane anesthesia. Cardiac blood samples were collected in heparinized tubes and centrifugated (1500 × g, 10 min, 4 °C) for collection of plasma. Terminal plasma samples were assayed for insulin and HbA1c. Insulin was measured in duplicates using an AlphaLisa kit (Perkin Elmer, Skovlunde, Denmark), according to the manufacturer's instructions. HbA1c was measured using commercial kits (Roche Diagnostics, Hvidovre, Denmark) on the Cobas c 501 autoanalyzer according to the manufacturer's instructions. *2.5. Simultaneous extraction of bacterial DNA and gut RNA*

Vehicle-dosed (n = 5) and rosiglitazone-treated (n = 6) mice were characterised for gut microbiome and transcriptome signatures. Segments (1 cm) from five individual gut regions (duodenum, jejunum, ileum, caecum and proximal colon) were dissected, snap frozen and stored at − 80 °C until further processing (Figs. 1,2 A). Simultaneous isolation of DNA and RNA from each individual gut sample was performed using ZymoBIOMICS DNA/RNA Miniprep Kit (ZYMO Research, Irvine, CA) to reduce bias associated with unequal lysis efficiency. In brief, with a FastPrep®-24 system samples were homogenized (1 min shaking every 2nd min, 5 cycles) in DNA/RNA Shield. The lysate was subsequently split and loaded onto two separate columns for DNA and RNA extraction. An in-column DNase I treatment step of RNA samples was included. A positive mock sample (ZymoBIOMICS Microbial Community Standard II (Log Distribution), ZYMO Research, Irvine, CA) served for control of DNA extraction efficiency.

2.6. Full-length 16S rRNA amplicon sequencing

500 ng of purified bacterial DNA from each sample served as template and was amplified by PCR (95 °C for 1 min, 29 × (95 °C for 20 s, 55 °C for 30 s, 65 °C for 2 min), 65 °C for 5 min) with 12 barcoding primers (16S Barcoding Kit, SQK-RAB204, Oxford Nanopore Technologies, Oxford, United Kingdom) targeting the ~1500 bp 16S rRNA gene, which is specific for bacteria. 16S DNA libraries were verified with both Qubit 4 Fluorometer (Thermo Fisher Scientific, Waltham, MA) and High Sensitivity DNA chips on a 2100 Bioanalyzer Instrument (Agilent Technologies, Santa Clara, CA). Four samples were excluded due to low bacterial content or sample contamination. Finalized 16S DNA libraries were pooled and prepared with a Flow Cell Priming Kit (EXP-FLP001, Oxford Nanopore Technologies) and loaded on a Flow Cell (FLO-MIN106D, Oxford Nanopore Technologies) onto a MinION Nanopore sequencer (Oxford Nanopore Technologies). Library pools had concentrations between 25.6–73.1 fmol. Sequencing runs ran for 6 h using the MinION control software MinKNOW (MinION Release 19.06.8). A positive DNA mock sample (ZymoBIOMICS Microbial Community DNA Standard II (Log Distribution)) was included in each round of library preparation to control for library size and PCR replicates.

2.7. Microbiome analysis

Nanopore sequencing raw FAST5 files were basecalled and demultiplexed by ONT Guppy basecalling software (v3.2.2) with default settings [30]. Samples with less than 25,000 reads were excluded, resulting in 46 samples for analysis. Passed reads were analysed downstream with Minimap2 (v2.17) and aligned to NCBI 16S rRNA gene database (version from 2019-09-05) identifying bacteria at genus level [31–33]. Single counts were removed, and samples were rarefied to an even depth with Phyloseq (v1.28.0) in R studios (R v3.6.0) [34]. Microbiome diversity and richness analysis was conducted as described previously [35,36].

2.8. Gene expression analysis using RNAseq

A total of 500 ng purified RNA from each sample was used to generate cDNA libraries using the NEBNext® Ultra™ II Directional RNA Library Prep Kit for Illumina (New England Biolabs, Ipswich, MA). Oligo dT-based mRNA isolation was used to specifically enrich for eukaryotic mRNAs. cDNA libraries were evaluated with Nanodrop (Thermo Fisher Scientific, Waltham, MA) and hereafter sequenced (75 base-pair, single- reads) on a NextSeq 500 using NextSeq 500/550 High Output Kit V2

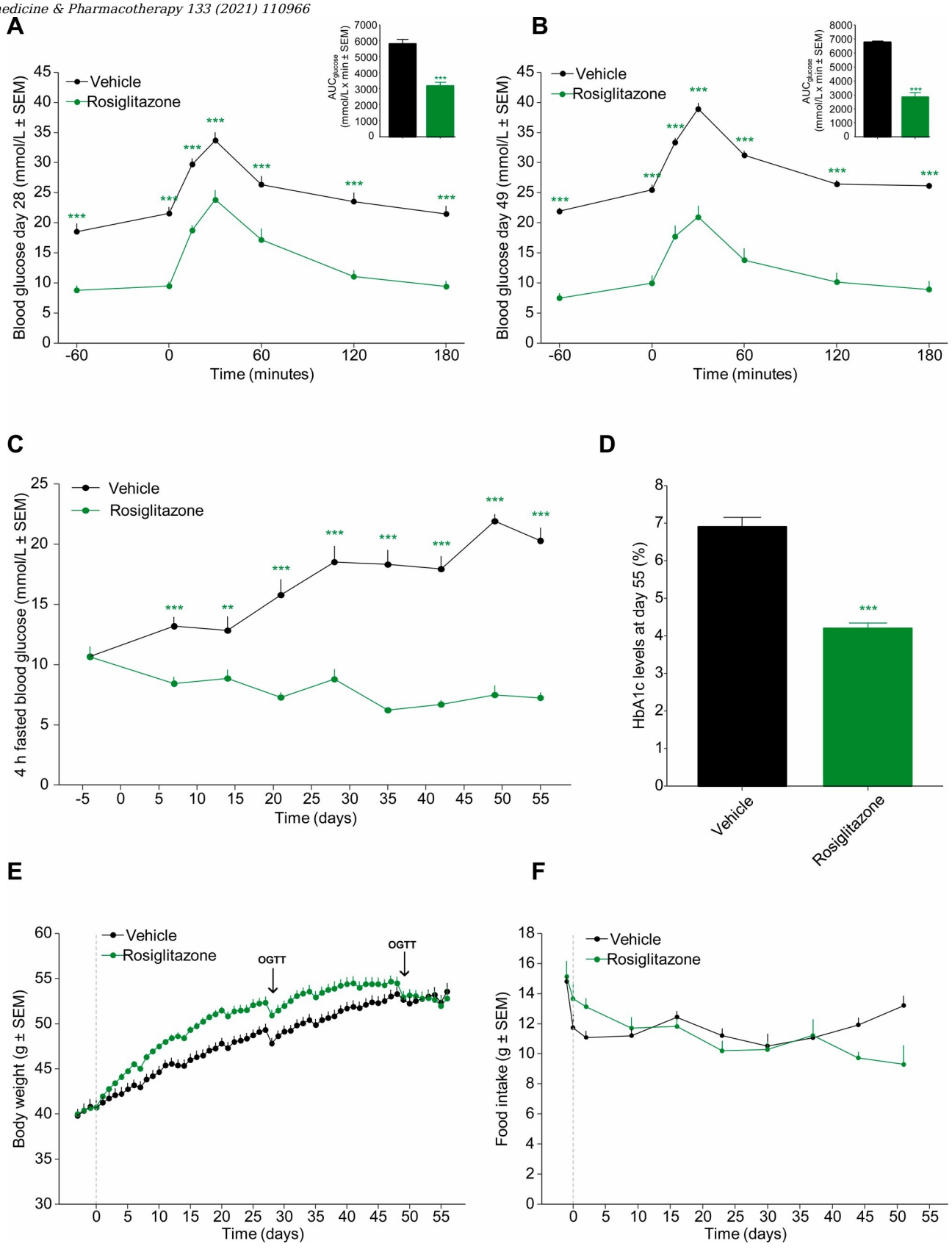

Fig. 1. Rosiglitazone improves metabolic parameters in *db/db* mice. (A) Oral glucose tolerance test (OGTT) on treatment day 28 and glucose area-under the-curve calculated from the OGTT glucose excursion curve; (B) Oral glucose tolerance test (OGTT) on treatment day 49 and glucose area-under the-curve calculated from the OGTT glucose excursion curve; (C) Weekly morning blood glucose concentrations (mmol/L), measured after four hours fasting; (D) Plasma HbA1c levels (%) at day 55; (E) Absolute body weight (g); (F) Daily food intake (g). **p < 0.01, ***p < 0.001 versus vehicle controls.

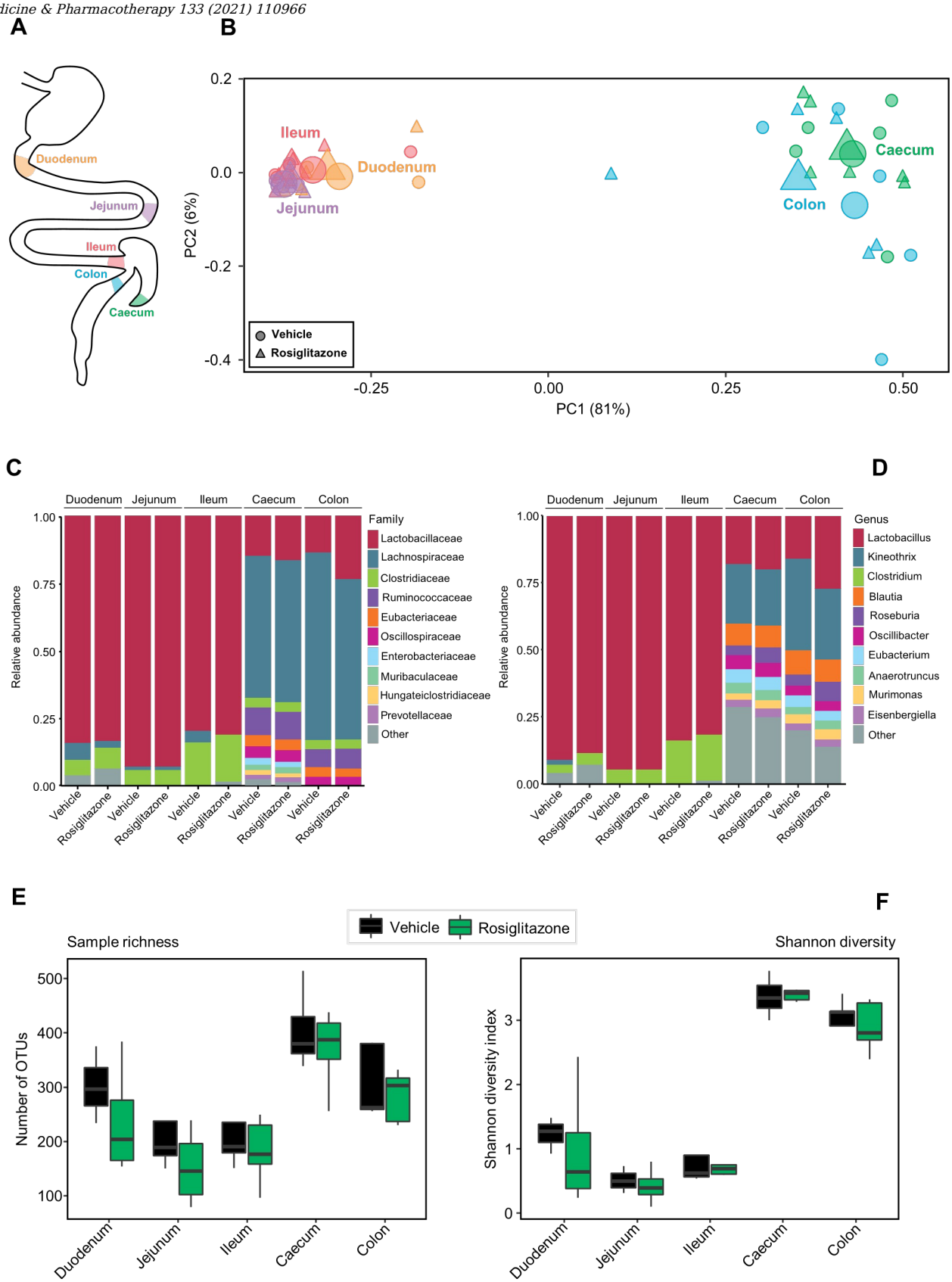

Fig. 2. Gut microbiome analysis of *db/db* mice by full-length 16S rRNA gene sequencing. (A) Outline of the murine gastrointestinal tract with delineation of gut segments sampled for analysis. (B) Principal Coordinate Analysis (PCoA) calculated by Bray-Curtis dissimilarity between samples based on rarefied data. Gut sections are coloured, and treatment groups shaped. Group means are indicated by a large point. Taxonomic summary of top 10 (C) families and (D) genera across all samples according to highest abundance and represented by mean values per group and gut section. Microbial alpha-diversity analysis at genus level illustrated by (E) richness and (F) Shannon diversity index.

(Illumina, San Diego, CA). A total of five RNA samples were excluded due to low RNA yields/ sample contamination/ RNA degradation. The resulting sequencing data was aligned to the mouse genome (GRCm38_96) obtained from the Ensembl database using the Spliced Transcripts Alignment to a Reference (STAR) (v2.5.0) software [37]. Data quality was evaluated using the standard RNA-sequencing quality control parameters; the inter- and intra-group variability was evaluated using principal component analysis (PCA) based on the 500 most variable genes, and hierarchical clustering. Differentially expressed genes (DEGs) were identified using the R-package DESeq2 [38] (v1.24.0). P-values were adjusted using the Benjamini-Hochberg method, and a cut-off of 0.05 (5% False Discovery Rate, FDR) was applied. The Reactome pathway database was retrieved and used as gene annotation for global transcriptional changes ($p < 0.05$). Reactome pathway analysis was performed with custom scripts employing a wide range of R packages, e.g. biomaRt, reshape2 (v1.4.3), roxygen2 and FactoMineR. Selected biological pathways were evaluated based on significant regulated genes. *2.9. Statistical analysis*

Statistical methods for microbiome and RNA sequencing analyses are indicated above. Blood biochemistry data were evaluated using a one- way ANOVA with Tukey's post-hoc test (glucose area-under-the curve (AUC), 4 -h fasted glucose, HbA1c, fasted insulin) or a two-way ANOVA with Bonferroni's multiple comparison test (body weight, food intake, OGTT glucose). A p-value less than 0.05 was considered statistically significant.

3. Results

3.1. Rosiglitazone improves insulin sensitivity in diabetic db/db mice

The two groups of *db/db* mice showed similar baseline body weight (vehicle, 40.8 ± 0.8 g; rosiglitazone 40.7 ± 0.2 g, p = 0.876), fasted blood glucose concentrations (vehicle, 10.7 ± 0.8 mmol/L; rosiglitazone 10.7 ± 0.8 mmol/L, p = 0.983) and HbA1c levels (vehicle, 4.7 ± 0.2 %; rosiglitazone 4.5 ± 0.1 %, p = 0.334). Plasma insulin levels remained stable throughout the entire dosing period in vehicle controls (baseline: 6999 ± 327 pg/mL; termination: 7628 ± 1076 pg/mL, p = 0.570) and rosiglitazone-treated db/db mice (baseline: 5988 ± 295 pg/mL; termination: 5718 ± 841 pg/mL, p = 0.741). Rosiglitazone significantly improved glucose excursions in two successive OGTTs performed on treatment day 28 ($p < 0.001$, Fig. 1 A) and 49 ($p < 0.001$, Fig. 1B). Rosiglitazone also improved weekly fasting blood glucose levels and terminal HbA1c levels ($p < 0.001$, Fig. 1C, D). Compared to vehicle dosing, rosiglitazone transiently increased daily body weight gain in *db/ db* mice (from treatment day 15–26, $p < 0.05$) without significantly affecting weekly food intake (Fig. 1 E, F).

3.2. Rosiglitazone does not influence local gut microbiome composition in diabetic db/db mice

Gut bacterial composition and host gene expression was analyzed in five individual gut segments of the *db/db* mouse (Fig. 2A). Dual bacterial DNA and host mRNA extraction was applied for direct comparison of gut microbial composition and host gene expression profiles. Rosiglitazone showed no significant effect on gut bacterial composition in *db/db* mice. A Principal Coordinate Analysis (PCoA) demonstrated that samples of the small intestine clustered closely together, i.e. displaying relatively low between-community diversity (beta-diversity) (Fig. 2B). Samples of the large intestine clustered less on PC2, signifying higher bacterial diversity between these samples. Thus, gut bacterial signatures were homogenous within individual gut segments of vehicle dosed *db/db* mice. Samples from the small intestine (duodenum, jejunum, and ileum) displayed more similar gut bacterial family and genera composition compared to samples from the large intestine (caecum and colon) (Fig. 2C, D). As determined by relative abundance at bacterial family level, *Lactobacillaceae* and *Lachnospiraceae* were predominant in the small and large intestine, respectively (Fig. 2C). While *Lactobacillus* was the most relatively abundant genus (>75 % of all genera) in the small intestine, the large intestine was characterized by more diverse genus composition predominantly composed by *Kineothrix*, *Lactobacillus* and *Blautia* (Fig. 2D). The large intestine showed more diverse bacterial composition as illustrated by increased sample richness and Shannon diversity (alpha-diversity) as compared to the small intestine (Fig. 2E, F).

3.3. Rosiglitazone displays gut segment-specific effects on gene expression

A global gene expression analysis in rosiglitazone-treated *db/db* mice indicated gut segment-specific changes in gene expression patterns compared to vehicle controls. Gene expression was largely unaffected in the duodenum of rosiglitazone-treated *db/db* mice (n = 3 differentially expressed genes (DEGs), $p < 0.05$), jejunum (n = 1 DEG, $p < 0.05$) and caecum (n = 20 DEGs, $p < 0.05$) (Fig. 3A). In contrast, rosiglitazone- treated *db/db* mice showed substantial changes in gene expression signatures in the ileum (n = 744 DEGs, $p < 0.05$) and colon (n = 833 DEGs, $p < 0.05$) with only a minor overlap between DEGs in the two gut segments (Fig. 3B). The RNA sequencing analysis indicated highly different transcriptome profiles across the five gut segments analyzed as illustrated by a principal component analysis (PCA) plot (Fig. 3C). PPAR-γ gene expression was detected throughout the gastrointestinal tract in vehicle-dosed *db/db* mice, showing highest expression in the colon (RPKM values ± SEM; duodenum 15.4 ± 8.7; jejunum 3.5 ± 0.6; ileum 6.7 ± 0.7; caecum 27.8 ± 7.7; colon 50.4 ± 3.3). Rosiglitazone treatment did not alter expression of PPAR-γ (RPKM values ± SEM; duodenum

12.6 ± 2.4; jejunum 3.4 ± 0.5; ileum 6.2 ± 0.6; caecum 23.6 ± 4.2; colon
40.2 ± 4.4. $p > 0.05$ compared to vehicle group).

Given that gene expression changes in rosiglitazone-treated *db/db* mice were largely confined to the ileum and colon, gene annotation maps were generated using the Reactome pathway database with focus on these two gut segments (Fig. 3D). Consistent with the marked changes in ileal and colonic global gene expression profiles, rosiglitazone-treated *db/db* mice displayed significant changes in several biological signaling pathways. DEGs were particular associated with Protein localization, Metabolism, and Immune system pathways (Fig. 3D). Perturbations in metabolic pathways were dominated by lipid metabolism-associated genes (Fig. 3E, 4C). While changes in Protein Localization and Lipid Metabolism pathways were most marked in the colon, the ileum showed more significant regulations linked to the Immune system (Figs. 3D, 4 D).

Considering the molecular target for rosiglitazone, transcriptome changes in the ileum and colon were probed for PPAR-associated transcriptional pathways, revealing a wide representation of PPAR-associated genes across the Reactome pathway categories (Fig. 4A). Accordingly, several DEGs implicated in peroxisomal proliferation (*Ppara*) protein import (*Cat, Ephx2, Pex14, Pex19, Slc27a2)* and peroxisomal fatty acid β-oxidation (*Abcd3, Acaa1a, Acaa1b, Acox1, Acox2, Crot, ECH1, Ehhadh, Hsd17b4)* were upregulated (Fig. 4A, C), indicating stimulation of PPAR-γ following long-term rosiglitazone treatment in diabetic *db/db* mice. In addition, rosiglitazone upregulated the expression of genes involved in mitochondrial β-oxidation and oxidative phosphorylation (*Acaa2*, *Cpt1a, Cpt2, Slc22a5, Slc25a20*). Notably, rosiglitazone stimulated fatty acid metabolism as indicated by regulation of genes involved in intestinal fatty acid absorption/transport (*Fabp1, Fabp2, Fabp5, Slc27a1, Slc27a2, Slc27a4*), synthesis (*Acacb, Acot12*) and degradation (*Chst11, Mgll, Pla2g6, Pla2g10, Plb1, Pnpla2*) (Fig. 4A, C). Furthermore, cytochrome genes linked to lipid metabolism (*Cyp4a10, Cyp2c66, Cyp4b1, Cyp2j6*) were significantly upregulated in the colon, but not in the ileum (Fig. 4C). A subset of DEGs were associated with glucose metabolism, including upregulation of genes

Fig. 3. RNA gene expression analysis of *db/db* gut sections. (A) Total number of differentially expressed genes in the five gut sections compared with vehicle at significance level ($p < 0.05$ after correction for multiple testing). (B) Venn diagram with genes regulated between treatment and vehicle specific to colon, ileum or shared between the two sections. (C) Principal Component Analysis (PCA) of the 500 most variable genes. The points indicate the relationship between samples across gene expression profiles. Gut sections are coloured, and treatment groups shaped. Group means are indicated by a large point. Whilst PC1 separates the small from the large intestine, PC2 clusters the individual gut segments demonstrating tissue-specific gene signatures. (D) Reactome pathways affected by rosiglitazone treatment. Pathways indicated in bold were further investigated (see Figure 4). (E) Reactome metabolism sub-pathways affected by rosiglitazone treatment.

Fig. 4. Rosiglitazone regulates genes involved in PPAR-γ signaling pathways. Heatmaps includes significantly regulated genes filtered based on an adjusted p-values smaller than 0.05 and a log2 fold change threshold with values above 1 or below -1. (A) Differential expressed genes (DEGs) which are direct PPAR targets; (B) DEGs involved in metabolism of carbohydrates; (C) DEGs involved in metabolism of lipids; (D) DEGs involved in the immune system. *$p < 0.05$, **$p < 0.01$, ***$p < 0.001$ versus vehicle controls (FDR adjusted p-values).

involved in gluconeogenesis (*Gpi1, Slc25a10, Slc37a2, Slc25a1*) and glycerol biogenesis (*Pdk4*) in the colon. In addition, rosiglitazone treatment resulted in downregulation of caecal and ileal genes involved in glycolysis (*Aldob*, *Eno1b*, *Hk1*) (Fig. 4B). In addition to metabolic pathways, immunomodulatory genes were regulated by rosiglitazone treatment, particularly markers associated with innate immune system responses. This includes genes associated with monocyte/macrophage function (*Cd68, C3ar1, Card9, Lyz2, Map3k8, Saa1*), B-cell (*Mme*) and T- cell activation (*Prkcq*), NK cells (*Fgfr3*) as well as enteric glial cells (*Gdnf*). Other regulated genes have been associated with antigen processing (*Asb11*), mucosal defense (*Cat, Slpi*) and the complement system (*C7, Colec10, C1s2, Fcna*). In addition, gut tight junction markers were investigated. Compared to vehicle controls, two colonic genes were significantly downregulated (*Mylk,* $p < 0.05$; *Jam2,* $p < 0.01$) and one ileal gene upregulated (*Jam2,* $p < 0.01$) following rosiglitazone treatment. All other tight junction-associated genes (*Cdh1, Cdh17, Cgn, Cldnd1, Cldn2, Cldn3, Cldn4, Cldn5, Cldn15, Cldn23, Ctnnb1, F11 r, Jam3, Jaml, Marveld2, Ocln, Tjp1, Tjp2, Tjp3)* were unaffected by treatment, irrespectively of the gut segment analysed.

4. Discussion

Rosiglitazone is an oral antidiabetic agent of the thiazolidinedione (TZD) class that improves glycaemic control primarily by increasing peripheral insulin sensitivity through selective activation of PPAR-γ particularly by stimulating gene expression programs that increase glucose uptake and improve insulin-stimulated glucose disposal [5,6]. Here, we report that long-term rosiglitazone treatment does not influence the gut microbiome profile in diabetic *db/db* mice while having profound effects on intestinal genes involved in nutrient metabolism.

This could suggest a contributory role of gut-derived PPAR-γ signalling in the metabolic effects of TZDs.

The small intestine plays a central role in nutrient absorption, digestion and immune function, whereas the proximal colon is primarily involved in water

absorption and fermentation of dietary fibres [39–41]. This makes it imperative to study local pharmacological effects on the gut microbiota composition, as analysis of the faecal microbiome closely reflects the microbiota profile of the distal colon only [42–44]. The present study profiled the microbiome composition across five different gut segments representing the entire rostro-caudal extension of the intestine in diabetic *db/db* mice. To avoid sample extraction bias, a dual DNA and mRNA purification kit was employed to enable direct comparison of local gut microbial composition and host gene expression profiles across the rostro-caudal extension of the gut. The simultaneous bacterial DNA-host mRNA isolation procedure enabled paired analysis of local gut microbiome and gut transcriptome signatures in rosiglitazone-treated *db/db* mice.

Recent studies have demonstrated discrete phylum/genus-level changes in the faecal gut microbiome in chow-fed *db/db* mice compared to chow-fed C57BL6 mice which are likely driven by hyperphagia [45,46]. Compared to vehicle-dosed *db/db* mice, rosiglitazone treatment did not influence gut segmental microbiome profiles in *db/db* mice. TZDs have previously been reported to have no effect on the faecal microbiome composition in DIO mice and rats [41,47], suggesting the intestinal microbiome may not play a contributory role in the metabolic effects of PPAR-γ agonists. On the other hand, the gut microbiota may modulate endogenous intestinal PPAR-γ activity which could have implications for nutrient metabolism. Accordingly, recent studies have demonstrated that PPAR-γ signalling in gut epithelial cells can be induced by short-chain fatty acids, the main metabolites produced by gut bacterial fermentation of dietary fibres [15,40,48,49]. Although there is increasing evidence that short-chain fatty acids and other microbial metabolites such as 3-indolepropionic acid and secondary bile acids have effects on host physiology, including energy/glucose metabolism, inhibition of microbial dysbiosis and protection of gut barrier function [12,50,51], it remains to be established whether gut PPAR-γ specifically contribute to these effects. The 16S sequencing analysis was limited to determine gut bacterial composition at the family/genus level in *db/db* mice, and it cannot be excluded that deeper sequencing may reveal discrete compositional changes at species level following rosiglitazone treatment in this type 2 diabetes model. Although the present dosing regimen significantly improved hyperglycemia in *db/db* mice, we cannot rule out that higher rosiglitazone doses or longer treatment duration could influence gut microbiome composition. As in the clinic, use of relatively high doses of rosiglitazone (≥10 mg/kg/day) is associated with significant weight gain in mice [52,53]. Given that weight gain is strongly associated with gut microbiome changes [29], it should be considered that higher doses may potentially influence gut microbiome composition related to the adverse, rather than therapeutic, effects of rosiglitazone.

Studies on intestinal transcriptional responses to PPAR-γ agonists, including rosiglitazone, have typically been limited to characterization of pre-selected genes [15,41,54–56]. To obtain further resolution of local gut effects of TZDs, we performed unsupervised analysis of gut segmental transcriptome changes following rosiglitazone treatment. In contrast to the lack of effect on the gut microbiome, rosiglitazone showed a marked effect on the intestinal gene expression profile in *db/db* mice, being largely localized to the ileum and colon. The significant colonic transcriptome changes were consistent with the colon showing highest expression of PPAR-γ. In the small intestine, ileal gene expression was responsive to rosiglitazone even though all segments of the small intestine displayed up to 10-fold lower PPAR-γ expression compared to the colon. Whether these effects may be explained by more effective PPAR-γ mediated signal transduction or ileal accumulation/uptake of rosiglitazone must await further studies.

PPAR-γ in adipose tissues is the primary target for the blood glucose- lowering effects of TZDs, predominantly through activation of adipocyte lipid flux and adipocyte differentiation whereby fat is sequestered away from insulin-resistant tissues such as skeletal muscle and the liver [57–59]. Also, stimulated adipokine release may play a role in the anti-diabetic effects of TZDs [60]. A large set of regulated intestinal genes in rosiglitazone-treated *db/db* mice were known PPAR-γ targets associated with gut lipid metabolism [56]. Consistent with PPAR-γ acting as a main gut lipid sensor [10,49], rosiglitazone treatment stimulated the expression of several gene markers of intestinal fatty acid uptake, transport and disposal. This effect was particularly observed in the colon which is consistent with PPAR-γ being abundantly expressed in colonic epithelial cells [13,14,56]. The implications of stimulated colonic PPAR-γ associated lipid metabolic signalling is unclear as the majority of lipid digestion and absorption occurs in the small intestine and only a small proportion of dietary fat reaches the large intestine [39, 61]. It should be emphasized that the colon is exposed to lipids derived from undigested dietary fat and to a lesser extent from endogenous secreted lipids and colonocytes shed at the gut epithelial surface [62]. In addition to dietary factors, short-chain fatty acids serve as important energy substrates for colonocytes [63]. It is possible that rosiglitazone also triggered lipid metabolism programs in non-parenchymal gut cell types. Accordingly, macrophages and dendritic cells are abundant in the gut [64,65], show high PPAR-γ receptor expression [66] and PPAR-γ receptors can activate fatty acid β-oxidation and triglyceride clearance in these immune cell subsets [67,68].

Intestinal gene expression profiles in rosiglitazone-treated *db/db* mice included regulation of ileal and colonic genes associated with carbohydrate metabolism. Although a subset of regulated genes encodes enzymes involved in gluconeogenesis and glycolysis, it should be noted that these enzymes are multifunctional and have diverse roles in e.g. cell migration and immune signaling [69,70]. The functional implications of these discrete changes are therefore unclear, however, may likely reflect local gut adaptive metabolic responses being unrelated to the glycaemic effects of rosiglitazone.

In addition to the prominent metabolic effects, intestinal PPAR-γ signalling controls the activity of several inflammatory response genes in epithelial cells, macrophages, dendritic cells and T-cells which is considered an important molecular mechanism for shaping gut immune responses to bacterial load and dietary immunogens [71,72]. Rosiglitazone has previously been demonstrated to exert intestinal anti-inflammatory effects [26,27]. Inflammatory tissue responses and gut dysbiosis have been demonstrated in obese and diabetic patients [73,74], however, a causal link between intestinal dysfunction and type 2 diabetes remains to be conclusively established. Impaired gut barrier integrity has been suggested to be an important driver of chronic low-grade inflammation in obesity and diabetes [75,76]. Accordingly, *db/db* mice have been reported to show indices of low-grade systemic inflammation, impaired gut barrier function and intestinal pro-inflammatory activity [45,50,77], which may potentially be linked to disrupted intestinal glucose transport and signaling [78,79]. Our study indicates that gene expression of tight junction components was largely unaffected by rosiglitazone treatment, which could suggest that gut barrier function did not contribute to the glucoregulatory effects of rosiglitazone in *db/db* mice. It should be noted that gut microbiome-host cross-talk at the level of immune cell signalling is important in both physiological and inflammatory conditions [19,21]. In the present study, oral rosiglitazone treatment altered the expression of immune gene markers, however, did not affect gut bacterial composition throughout the gut in *db/db* mice. In combination, this argues for gut microbiota-independent immunomodulatory effects of rosiglitazone and suggests a potential therapeutic role for TZDs in metabolic gut inflammatory diseases

5. Conclusion

Rosiglitazone improves glucose homeostasis without altering the gut microbiome composition in diabetic *db/db* mice. Rosiglitazone promoted marked changes in local intestinal transcriptome signatures of metabolic reprogramming towards increased intestinal lipid utilization and altered gut immune signalling, which could suggest that rosiglitazone may potentially improve local gut metabolic function associated with diabetes.

Funding

This study was supported by a grant from Innovation Fund Denmark (M.S.M., grant no. 7038-00008B).

Authors contributions statement

Conceived and designed the experiments: R.V.G, J.E., M.S.M, J.J., N. V. and M.M.; performed the experiments: M.S.M and M.C.D; analyzed and interpreted the data: M.S.M., K.R., M.R.M, M.M., J.J. and H.H.H.; wrote the manuscript: M.S.M., M.M., M.S., J.J. and H.H.H. All authors have read and approved the final manuscript.

Data availability statement

All data generated or analyzed during this study are included in this published article.

Declaration of Competing Interest

M.S.M., R.V.G., M.C.D., K.R., M.R.M., H.H.H. and M.M. are employed by Gubra; N.V. and J.J. are owners of Gubra. J.E. is co-founder of Pendulum.

References

[1] S.A. Montandon, F.R. Jornayvaz, Effects of antidiabetic drugs on gut microbiota composition, Genes (Basel) 8 (2017).
[2] M. Zimmermann, M. Zimmermann-kogadeeva, R. Wegmann, A.L. Goodman, Separating host and microbiome contributions to drug pharmacokinetics and toxicity, Sci. Drug Metab. 363 (2019).
[3] R.K. Weersma, A. Zhernakova, J. Fu, Interaction between drugs and the gut microbiome, Gut 0 (2020) 1–10.
[4] A. Vich Vila, et al., Impact of commonly used drugs on the composition and metabolic function of the gut microbiota, Nat. Commun. 11 (2020) 1–11.
[5] L. Lipscombe, et al., Guidelines for the prevention and management of diabetes in Canada: pharmacologic glycemic management of type 2 diabetes in adults, Can. J. Diabetes 42 (2018) S88–S103.
[6] M.A. Davidson, et al., Thiazolidinedione drugs in the treatment of type 2 diabetes mellitus: past, present and future, Crit. Rev. Toxicol. 48 (2018) 52–108.
[7] R.T. Nolte, et al., Ligand binding and co-activator assembly of the peroxisome proliferator- activated receptor-γ, Nature 395 (1998) 137–143.
[8] J. Berger, D.E. Moller, The mechanisms of action of PPARs, Annu. Rev. Med. 53 (2002) 409–435.
[9] J.P. Berger, T.E. Akiyama, P.T. Meinke, PPARs: Therapeutic targets for metabolic disease, Trends Pharmacol. Sci. 26 (2005) 244–251.
[10] L. Poulsen, C. la, M. Siersbæk, S. Mandrup, PPARs: fatty acid sensors controlling metabolism, Semin. Cell Dev. Biol. 23 (2012) 631–639.
[11] P. Desreumaux, et al., Attenuation of colon inflammation through activators of the retinoid X receptor (RXR)/peroxisome proliferator-activated receptor γ (PPARγ) heterodimer: a basis for new therapeutic strategies, J. Exp. Med. 193 (2001) 827–838.
[12] M. Nepelska, et al., Commensal gut bacteria modulate phosphorylation-dependent PPARγ transcriptional activity in human intestinal epithelial cells, Sci. Rep. 7 (2017) 1–13.
[13] A. Mansen, H. Guardiola-Diaz, J. Rafter, C. Branting, J.Å. Gustafsson, Expression of´ the peroxisome proliferator-activated receptor (PPAR) in the mouse colonic mucosa, Biochem. Biophys. Res. Commun. 222 (1996) 844–851.
[14] A.M. Lefebvre, et al., Peroxisome proliferator-activated receptor gamma is induced during differentiation of colon epithelium cells, J. Endocrinol. 162 (1999) 331–340.
[15] M.X. Byndloss, et al., Microbiota-activated PPAR-γ signaling inhibits dysbiotic Enterobacteriaceae expansion, Science (80-.) 357 (2017) 570–575.
[16] A. Ul Hasan, A. Rahman, H. Kobori, Interactions between host PPARs and gut microbiota in health and disease, Int. J. Mol. Sci. 20 (2019).
[17] C.J. Kelly, et al., Crosstalk between microbiota-derived short-chain fatty acids and intestinal epithelial HIF augments tissue barrier function, Cell Host Microbe 17 (2015) 662–671.
[18] L. Dubuquoy, et al., PPARγ as a new therapeutic target in inflammatory bowel diseases, Gut 55 (2006) 1341–1349.
[19] G. Hajishengallis, J.D. Lambris, Microbial manipulation of receptor crosstalk in innate immunity, Nat. Rev. Immunol. 11 (2011).
[20] R.J. Xavier, D.K. Podolsky, Unravelling the pathogenesis of inflammatory bowel disease, Nat. Rev. 448 (2007) 427–434.
[21] D. Zheng, T. Liwinski, E. Elinav, Interaction between microbiota and immunity in health and disease, Cell Res. (2020), https://doi.org/10.1038/s41422-020-0332-7.

[22] C.G. Su, et al., A novel therapy for colitis utilizing PPAR-γ ligands to inhibit the epithelial inflammatory response, J. Clin. Invest. 104 (1999) 383–389.
[23] B.M. Necela, E.A. Thompson, Pathophysiological roles of PPARγ in gastrointestinal epithelial cells, PPAR Res. 2008 (2008).
[24] C.S. Eun, D.S. Han, S.H. Lee, C.H. Paik, Attenuation of colonic inflammation by PPAR γ in intestinal epithelial cells : effect on toll-like receptor pathway, Dig. Dis. Sci. 51 (2006) 693–697.
[25] D. Kelly, et al., Commensal anaerobic gut bacteria attenuate inflammation by regulating nuclear-cytoplasmic shuttling of PPAR- γ and RelA, Nat. Immunol. 5 (2004) 104–112.
[26] M. Adachi, et al., Peroxisome proliferator activated receptor γ in colonic epithelial cells protects against experimental inflammatory bowel disease, Gut 55 (2006) 1104–1113.
[27] K. Celinski, et al., Comparison of anti-inflammatory properties of peroxisome proliferator-activated receptor gammaagonists rosiglitazone and troglitazone in prophylactic treatment of experimental colitis, J. Physiol. Pharmacol. 64 (2013) 587–595.
[28] P.J. Turnbaugh, et al., A core gut microbiome in obese and lean twins, Nature 457 (2009) 480–484.
[29] R.E. Ley, et al., Obesity alters gut microbial ecology, PNAS 102 (2005) 11070–11075.
[30] R.R. Wick, L.M. Judd, K.E. Holt, Performance of neural network basecalling tools for Oxford Nanopore sequencing, Genome Biol. 20 (2019) 1–10.
[31] H. Li, Minimap2: Pairwise alignment for nucleotide sequences, Bioinformatics 34 (2018) 3094–3100.
[32] N.A. O'Leary, et al., Reference sequence (RefSeq) database at NCBI: current status, taxonomic expansion, and functional annotation, Nucleic Acids Res. 44 (2016) D733–D745.
[33] T. Tatusova, S. Ciufo, B. Fedorov, K. O'Neill, I. Tolstoy, RefSeq microbial genomes database: new representation and annotation strategy, Nucleic Acids Res. 42 (2014) 553–559.
[34] B.J. Callahan, K. Sankaran, J.A. Fukuyama, P.J. McMurdie, S.P. Holmes, Bioconductor workflow for microbiome data analysis: from raw reads to community analyses [version 1; referees: 3 approved], F1000Research 5 (2016) 1–48.
[35] M.S.A. Madsen, et al., Metabolic and gut microbiome changes following GLP-1 or dual GLP-1/GLP-2 receptor agonist treatment in diet-induced obese mice, Sci. Rep. 9 (2019) 15582.
[36] E.K. Morris, et al., Choosing and using diversity indices: insights for ecological applications from the German biodiversity exploratories, Ecol. Evol. 4 (2014) 3514–3524.
[37] A. Dobin, et al., STAR: ultrafast universal RNA-seq aligner, Bioinformatics 29 (2013) 15–21.
[38] M.I. Love, S. Anders, W. Huber, Differential analysis of count data - the DESeq2 package, Genome Biol. 15 (2014).
[39] R. Bowcutt, et al., Heterogeneity across the murine small and large intestine, World J. Gastroenterol. 20 (2014) 15216–15232.
[40] H.Y.P. Oh, V. Visvalingam, W. Wahli, The PPAR-microbiota-metabolic organ trilogy to fine-tune physiology, FASEB J. 33 (2019) 9706–9730.
[41] J. Tomas, et al., High-fat diet modifies the PPAR-γ pathway leading to disruption of microbial and physiological ecosystem in murine small intestine, Proc. Natl. Acad. Sci. U. S. A. 113 (2016) E5934–E5943.
[42] F. Sommer, I. Nookaew, N. Sommer, P. Fogelstrand, F. Backhed, Site-specific¨ programming of the host epithelial transcriptome by the gut microbiota, Genome Biol. 16 (2015) 1–15.
[43] R.B. Jones, et al., Inter-niche and inter-individual variation in gut microbial community assessment using stool, rectal swab, and mucosal samples, Sci. Rep. 8 (2018) 1–12.
[44] K. Martinez-Guryn, V. Leone, E.B. Chang, Regional diversity of the gastrointestinal microbiome, Cell Host Microbe 26 (2019) 314–324.
[45] W. Zhang, J.H. Xu, T. Yu, Q.K. Chen, Effects of berberine and metformin on intestinal inflammation and gut microbiome composition in db/db mice, Biomed. Pharmacother. 118 (2019).
[46] R. Nagpal, S.P. Mishra, H. Yadav, Unique gut microbiome signatures depict diet- versus genetically induced obesity in mice, Int. J. Mol. Sci. 21 (2020) 3434.
[47] J. Bai, Y. Zhu, Y. Dong, Response of gut microbiota and inflammatory status to bitter melon (Momordica charantia L.) in high fat diet induced obese rats, J. Ethnopharmacol. 194 (2016) 717–726.
[48] S. Alex, et al., Short-chain fatty acids stimulate angiopoietin-like 4 synthesis in human Colon adenocarcinoma cells by activating peroxisome proliferator-activated receptor, Mol. Cell. Biol. 33 (2013) 1303–1316.
[49] P.A. Grimaldi, Peroxisome proliferator-activated receptors as sensors of fatty acids and derivatives, Cell. Mol. Life Sci. 64 (2007) 2459–2464.
[50] Y. Wang, et al., Composite probiotics alleviate type 2 diabetes by regulating intestinal microbiota and inducing GLP-1 secretion in db/db mice, Biomed. Pharmacother. 125 (2020), 109914.
[51] E. Amabebe, F.O. Robert, T. Agbalalah, E.S.F. Orubu, Microbial dysbiosis-induced obesity: role of gut microbiota in homoeostasis of energy metabolism, Br. J. Nutr. 123 (2020) 1127–1137.
[52] L. Zhou, et al., Increased susceptibility of db/db mice to rosiglitazone-induced plasma volume expansion: role of dysregulation of renal water transporters, Am. J. Physiol. - Ren. Physiol. 305 (2013).
[53] E. Chaput, R. Saladin, M. Silvestre, A.D. Edgar, Fenofibrate and rosiglitazone lower serum triglycerides with opposing effects on body weight, Biochem. Biophys. Res. Commun. 271 (2000) 445–450.
[54] G. D'Argenio, et al., Colon OCTN2 gene expression is up-regulated by peroxisome proliferator-activated receptor γ in humans and mice and contributes to local and systemic carnitine homeostasis, J. Biol. Chem. 285 (2010) 27078–27087.
[55] J. Zhao, R. Zhao, L. Cheng, J. Yang, L. Zhu, Peroxisome proliferator-activated receptor gamma activation promotes intestinal barrier function by improving mucus and tight junctions in a mouse colitis model, Dig. Liver Dis. 50 (2018) 1195–1204.
[56] W. Su, et al., Differential expression, distribution, and function of PPAR-γ in the proximal and distal colon, Physiol. Genomics 30 (2007) 342–353.
[57] A. Okuno, et al., Troglitazone increases the number of small adipocytes without the change of white adipose tissue mass in obese Zucker rats, J. Clin. Invest. 101 (1998) 1354–1361.
[58] W. He, et al., Adipose-specific peroxisome proliferator-activated receptor γ knockout causes insulin resistance in fat and liver but not in muscle, Proc. Natl. Acad. Sci. U. S. A. 100 (2003) 15712–15717.
[59] G. Martin, K. Schoonjans, B. Staels, J. Auwerx, Pparγ activators improve glucose homeostasis by stimulating fatty acid uptake in the adipocytes, Atherosclerosis 137 (1998). Elsevier Ireland Ltd.
[60] M. Bouskila, U.B. Pajvani, P.E. Scherer, Adiponectin: a relevant player in PPARγ- agonist-mediated improvements in hepatic insulin sensitivity? Int. J. Obes. 29 (2005) S17–S23.
[61] C.W. Ko, J. Qu, D.D. Black, P. Tso, Regulation of intestinal lipid metabolism: current concepts and relevance to disease, Nat. Rev. Gastroenterol. Hepatol. 17 (2020) 169–183.
[62] L. Hoyles, J. Wallace, Gastrointestinal tract: fat metabolism in the colon, in: T. McGenity, K.N. Timmis, J.A. van der Meer, V. De Lorenzo (Eds.), Handbook of Hydrocarbon and Lipid Microbiology, 4, Springer, 2009, pp. 3114–3117. Part 7.
[63] J.M.W. Wong, R. De Souza, C.W.C. Kendall, A. Emam, D.J.A. Jenkins, Colonic health: fermentation and short chain fatty acids, J. Clin. Gastroenterol. 40 (2006) 235–243. J Clin Gastroenterol.
[64] E.R. Mann, et al., Compartment-specific immunity in the human gut: properties and functions of dendritic cells in the colon versus the ileum, Gut 65 (2016) 256–270.
[65] C.C. Bain, et al., Resident and pro-inflammatory macrophages in the colon represent alternative context-dependent fates of the same Ly6C hi monocyte precursors, Mucosal Immunol. 6 (2013) 498–510.
[66] D.S. Straus, C.K. Glass, Anti-inflammatory actions of PPAR ligands: new insights on cellular and molecular mechanisms, Trends Immunol. 28 (2007) 551–558.
[67] M.N. Xavier, et al., PPARγ-mediated increase in glucose availability sustains chronic brucella abortus infection in alternatively activated macrophages, Cell Host Microbe 14 (2013) 159–170.

[68] L. Nagy, A. Szanto, I. Szatmari, L. Sz´eles, Nuclear hormone receptors enable macrophages and dendritic cells to sense their lipid environment and shape their immune response, Physiol. Rev. 92 (2012) 739–789.
[69] V.M. Corrigall, G.S. Panayi, Autoantigens and immune pathways in rheumatoid arthritis, Crit. Rev. Immunol. 22 (2002) 281–293.
[70] A.J. Wolf, et al., Hexokinase is an innate immune receptor for the detection of bacterial peptidoglycan, Cell 166 (2016) 624–636.
[71] L. Peyrin-Biroulet, et al., Peroxisome proliferator-activated receptor gamma activation is required for maintenance of innate antimicrobial immunity in the colon, Proc. Natl. Acad. Sci. U. S. A. 107 (2010) 8772–8777.
[72] A.J. Guri, S.K. Mohapatra, W.T. Horne, R. Hontecillas, J. Bassaganya-Riera, The Role of T cell PPAR γ in mice with experimental inflammatory bowel disease, BMC Gastroenterol. 10 (2010).
[73] K.E. Wellen, G.S. Hotamisligil, Inflammation, stress, and diabetes, J. Clin. Invest. 115 (2005) 1111–1119.
[74] H. Tilg, N. Zmora, T.E. Adolph, E. Elinav, The intestinal microbiota fuelling metabolic inflammation, Nat. Rev. Immunol. 20 (2020) 40–54.
[75] P.D. Cani, et al., Metabolic endotoxemia initiates obesity and insulin resistance, Diabetes 56 (2007) 1761–1772.
[76] C. Sorini, et al., Loss of gut barrier integrity triggers activation of islet-reactive T cells and autoimmune diabetes, Proc. Natl. Acad. Sci. U. S. A. 116 (2019) 15140–15149.
[77] Y.H. Xu, et al., Sodium butyrate supplementation ameliorates diabetic inflammation in db/db mice, J. Endocrinol. 238 (2018) 231–244.
[78] T. Duparc, et al., Jejunum inflammation in obese and diabetic mice impairs enteric glucose detection and modifies nitric oxide release in the hypothalamus, Antioxidants Redox Signal. 14 (2011) 415–423.
[79] C.A. Thaiss, et al., Hyperglycemia Drives Intestinal Barrier Dysfunction and Risk for Enteric Infection, 359, 2018, pp. 1376–1383.